A Novel Ergonomic Upper-Limb Exoskeleton to Reduce Workers' Physical Strain

An Experimental Evaluation of the Proto-MATE

©ISTOCKPHOTO.COM/GERENME

By Ilaria Pacifico, Alessandro Scano, Eleonora Guanziroli, Matteo Moisé, Luca Morelli, Andrea Chiavenna, Duane Romo, Stefania Spada, Giuseppe Colombina, Franco Molteni, Francesco Giovacchini, Nicola Vitiello, and Simona Crea

Wearable passive upper-limb exoskeletons have been proposed and commercialized as tools to improve the ergonomics of workers in repetitive or physically demanding tasks. In the study presented here, an innovative upper-limb exoskeleton is presented, along with experimental tests with human subjects. The device, called *proto-MATE*, is characterized by two distinguishing design features: a highly ergonomic human–robot kinematics architecture and bioinspired assistance, created to partially compensate for the user's arm weight. Experimental tests investigated the device's effects on the physical strain of eight upper-limb muscles. These tests also quantified the kinematic coupling between the device and the user by means of specific kinematics-related parameters. The protocol included overhead tasks that are representative of the target application and tasks that generalize nontargeted upper-limb movements and may occur in real working conditions.

The results obtained from 15 individuals showed that using the proto-MATE can reduce electromyography (EMG)

Digital Object Identifier 10.1109/MRA.2019.2954105
Date of current version: 7 January 2020

activations of the upper-limb muscles by up to 43%. Significant reductions were observed for most upper-limb muscles involved in flexion movements and shoulder stabilization, particularly the anterior deltoid, medial deltoid, trapezius ascendens, and pectoralis major. The shoulder's ranges of motion for abduction–adduction and flexion–extension were not significantly altered when using the proto-MATE, and the human–robot relative displacement during the tasks was always lower than 2 mm, thus proving a stable and reliable human–robot kinematics coupling. Further longitudinal studies with workers are needed to investigate the long-term effects of using the device on the incidence of work-related musculoskeletal disorders (WRMDs).

Background

According to the Sixth European Working Conditions Survey, WRMDs are the most common occupational illnesses in Europe. Indeed, nearly 50% of European workers (75–80 million) suffer from back, neck, or upper-limb disorders [1], causing significant health and cost issues [2].

These health issues cause a huge financial burden for companies and healthcare systems. Indeed, companies must manage the costs of replacing and training workers as well as the related reduced productivity, while healthcare systems need to address the costs for all compensation claims made [2].

To reduce exposure to the risk factors of musculoskeletal injuries, three main courses of actions can be considered: 1) redesigning the workplace (e.g., optimizing the labor environment to enable working in a comfortable, strain-free posture); 2) integrating job rotations; and 3) introducing practices such as training for workers or periodic rest periods. Despite the approaches mentioned, repetitive movements, awkward postures, overexertion, and vibration can still cause a significant number of WRMDs. Most disorders on record are related to repetitive movements (which account for 61% of the workers); of these, 44% are related to overhead tasks [3] and awkward body postures (which account for 43% of WRMDs cases) [1].

Substituting humans with robots in repetitive tasks related to upper-limb activities would seem like a possible solution to safeguard humans from performing strenuous and repetitive movements while maintaining productivity. However, many specific tasks involving shoulder elevation require high flexibility and versatility, and fully automated solutions are not yet feasible. In the last few years, several companies started to develop and commercialize gravity-assistive, wearable upper-limb exoskeletons to improve conditions for workers and follow the recommendations provided by European Union legislations in terms of assessing and reducing workers' ergonomics risks (e.g., UNI EN 1005-4 related to incongruent postures and UNI EN 1005-pr5 related to repetitive handling at high frequency).

Given the strict health and safety requirements with which any industrial equipment must comply and considering several psychological and physical barriers, most companies opted to develop passive devices. Examples of commercially available upper-limb passive exoskeletons for workers are EksoVest (EksoBionics, Richmond, California), Airframe (Levitate Technologies, San Diego, California), ShoulderX (SuitX Emeryville, California), PAEXO (Ottobock, Duderstadt, Germany), and Skel'Ex (Skel'Ex, Rotterdam, The Netherlands).

Typically, the effects of upper-limb exoskeletons for worker applications have been evaluated in tests where users perform specific tasks that simulate potential applications (i.e., light assembly, overhead drilling, wiring, or painting). In these scenarios, the metrics most often used to verify the device's effectiveness in reducing users' physical demands relate to the reduced activity of the assisted muscles [4]–[7]. In some cases, improvements in the precision and quantity of work tasks have been reported as effectiveness-related metrics [8]. In addition to effectiveness metrics, Theurel et al. [7] and Kim et al. [5] investigated potential alterations of the arm kinematics or body posture while standing or walking with the device as a way to verify potential undesired effects of the exoskeletons. With the same objective, Van Engelhoven et al. [6] and Theurel et al. [7] measured the biomechanical strain on unassisted muscles. Several studies also reported on subjective evaluations of the device, by means of acceptance questionnaires [e.g., the Technology Acceptance Model (TAM) and TAM2 [8]] and usability questionnaires (the System Usability Scale). In some studies, the perceived discomfort of selected body parts and the overall perceived workload when executing the task (NASA Task Load Index) were also considered [5].

The MATE was designed to provide a compact design thus minimizing the risk of entrapment and entanglement with parts of the external environment.

We present and evaluate a novel passive exoskeleton designed to provide upper-limb support to workers in overhead tasks and repetitive upper-limb movements. The device is characterized by two distinguishing design features: a highly ergonomic human–robot kinematics interaction and bioinspired assistance. The human–robot kinematic coupling results from the combination of the physical human–machine interface (pHMI), a kinematic chain of passive degrees of freedom (pDOF), and several size regulations. All of these components ensure the device fits properly and the human and robot joint axes self-align smoothly, thus distributing and minimizing the transfer of parasitic forces to the user at contact points. The assistive profile matches the biological gravitational angle–torque profile of the upper limbs, providing a smooth partial gravity compensation that reduces the load on upper-limb muscles, particularly those in the shoulder, involved in elevation movements.

The exoskeleton presented and tested in this study is a premarket version of the muscular aiding tech exoskeleton (MATE), a device commercialized by COMAU S.p.A. [20]. It was designed and developed by IUVO SRL [21] in collaboration with COMAU S.p.A., Össur hf [22], and the Ergo Lab team of Fiat Chrysler Automobiles, with the goal of assisting workers in the final assembly of underbody operations (Figure 1). To address the specific requirements of the automotive sector, along with the bioinspired assistance strategy and ability to faithfully mimic shoulder kinematics, the MATE was designed to provide a compact design, i.e., with no protruding components, thus minimizing the risk of entrapment and entanglement with parts of the external environment.

Notably, the MATE prototype, called *proto-MATE* in this study, is functionally equivalent to the MATE; few elements have been modified in the market version to improve the system's adjustability for users and increase the components' mechanical durability and manufacturability. In this article, along with a description of the proto-MATE, we present the results of its first experimental evaluation. To assess the device's effectiveness and potential undesired effects, we designed an evaluation protocol that included tasks representative of the target application and tasks generalizing untargeted upper-limb movements that may occur in real working conditions.

In addition to a comprehensive set of tasks that generalize many upper-limb movements, this study proposes to evaluate the effects of the proto-MATE device by means of EMG indicators, calculated on several upper-limb muscles and by means of gauges that quantify the human–robot kinematics coupling, to quantify the effects of the exoskeleton on the physiological movement of the shoulder.

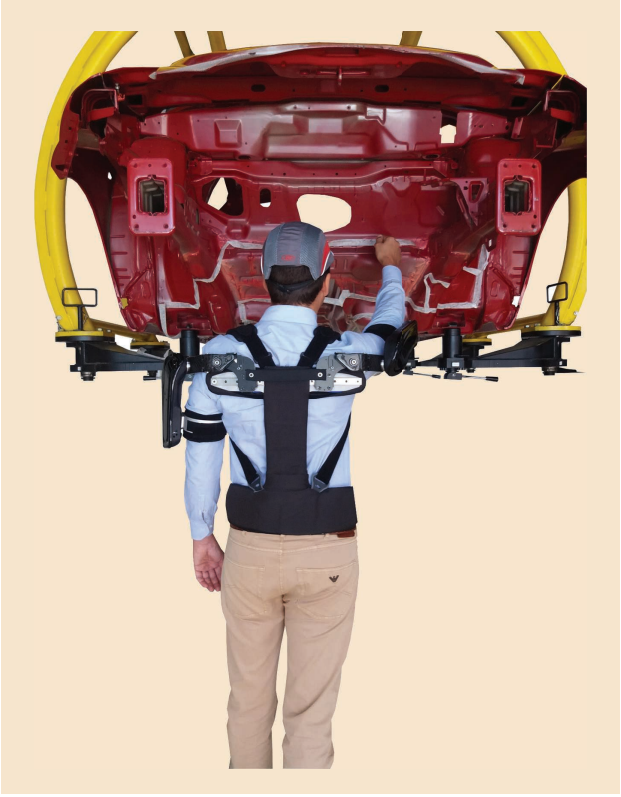

Figure 1. An operator wearing the proto-MATE in a simulated automotive underbody scenario.

System Design

Figure 2(a) shows the proto-MATE worn by a user. The device has a total weight of 3.5 kg and is made up of four main components:

1) the torque generator boxes that produce the gravitational torque to support the arms' weight
2) the pHMI, which connects the device to the human body at the waist, trunk, and arms and is responsible for transferring the forces to the human body and supporting the reaction forces
3) the kinematic chain of pDOF, which is responsible for self-aligning the robotic and human joint axes
4) a set of size regulations that allow adjusting the exoskeleton to fit users with different anthropometries.

The design of the proto-MATE is patent pending [9].

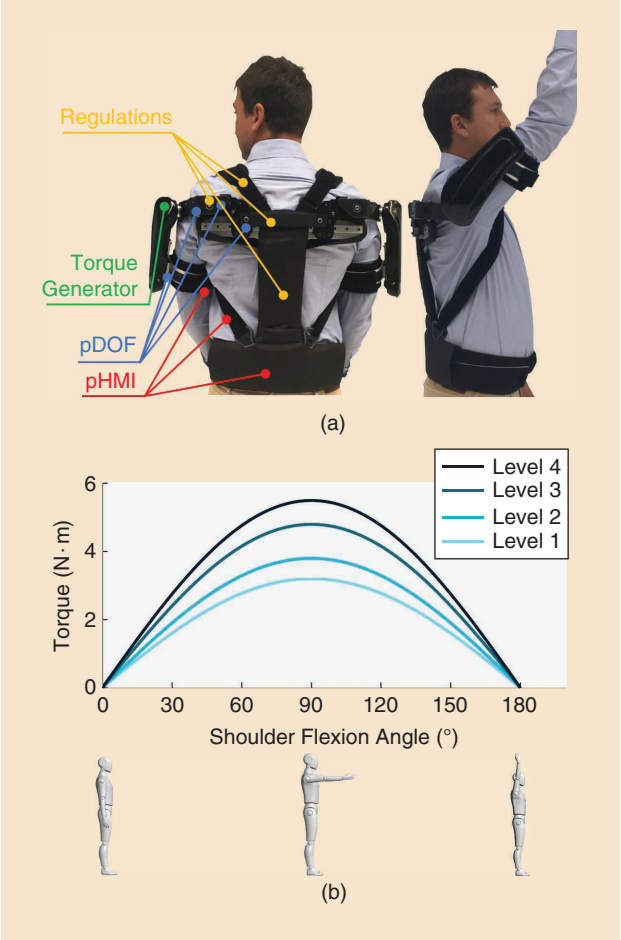

Figure 2. An overview of the proto-MATE. (a) The back and lateral views of the device. (b) The assistive torque profiles with four levels of assistance (i.e., levels 1, 2, 3, and 4 are set to compensate for up to 3.2, 3.8, 4.8, and 5.5 N·m, respectively, of the maximum gravitational torque).

Torque Generator Box

Torque generator boxes are the passive actuation units that store and transform the elastic energy of a set of two parallel springs into assistive action. The compensation system comprises two connected gears, of which one is coupled with the shoulder joint and the other is not concentrically bonded to the set of springs. The described mechanism is arranged in such a way that, when the arm lays parallel to the trunk, the spring force reaches its maximum value, and the moment arm is null with respect to the spring gear axis, thus generating null torque. As the arm elevation increases, the elastic force decreases but the moment arm increases: this mechanism generates a resulting torque that consistently varies with the gravity torque profile of the arm in a physiological shoulder elevation. Hence, the maximum assistive torque value is reached when the arm's elevation angle is at 90°, and it gradually goes to zero when the arm is relaxed. The proto-MATE allows tuning the assistive torque over four discrete levels [Figure 2(b)].

pHMI

The pHMI consists of the back-support structure and all parts that connect the device with the user's body, such as the shoulder straps, the arm cuffs, and the belt. The back-support structure is an aluminum frame molded in a T shape and is designed to distribute the reaction forces produced by the torque generator boxes to the user's pelvic area through a custom belt.

Kinematic Chain of pDOFs

A kinematic pDOF chain was designed to enable self-alignment of the device's joint axes to the human joint axes, minimizing the transfer of undesired forces to the user's musculoskeletal system. The entire pDOF chain enables the system to freely abduct/adduct the arm and smoothly counteract the passive medial–lateral and antero–posterior (AP) translational movements of the glenohumeral joint that occur when abducting or elevating the arm [10], [11]. The passive mechanical chain is symmetrical to the sagittal plane: on each side, a horizontal slider is connected in series to two rotational joints with mutually perpendicular axes. The first joint should be aligned with the shoulder abduction–adduction axis, while the second has a vertical axis that is not coupled with any specific biological axis and whose action, combined with the horizontal slider, accounts for the passive AP movement of the glenohumeral joint. An additional passive slider is placed between the active box and the arm cuff, to absorb the undesired translational longitudinal reaction forces at the arm–cuff interface.

Size Regulations

To fulfill the ergonomic requirements for safe and effective human–machine fitting and interaction, additional size regulations have been designed to adjust the height of the back frame and the width of the device, tune the orientation of the actuation boxes on the frontal plane, and adjust the length of the shoulder straps. Additional adjustments permit tightening the pelvic belt and adjusting the shoulder straps each time the exoskeleton is worn.

Experimental Session

Participants

The experiments took place at the Villa Beretta Rehabilitation Center, Valduce Hospital, in Lecco, Italy. Fifteen healthy subjects (of which 11 were men) were recruited for this study (32 ± 9 years, 72 ± 12 kg, 176 ± 6 cm). All participants had no prior experience with the exoskeleton. Subjects who had skin wounds in areas on which the device is applied or had a height outside the required range (160–195 cm) were not enrolled in this study.

Torque generator boxes are the passive actuation units that store and transform the elastic energy of a set of two parallel springs into assistive action.

Experiments were conducted in accordance with the Declaration of Helsinki, and the protocol was approved by the Institutional Ethics Committee of Insubria (study 154 of 2017). Subjects were informed about the study's general purpose and signed a written informed consent.

Data Recordings

Muscular activity was monitored using the Free EMG 1000 from BTS Bioengineering. Surface EMG electrodes (silver-silver chloride electrodes, Ambu WhiteSensor, 36 mm) were placed over the shoulder muscles following the Surface EMG for the Non-Invasive Assessment of Muscles recommendations [12]. Electrodes were placed unilaterally on the right limb and on the following muscles: anterior deltoid, medial deltoid, posterior deltoid, pectoralis major, latissimus dorsi, biceps brachii long head, triceps brachii long head, and trapezius ascendens. Electrodes were secured to the user's skin with medical tape, and signals were checked by the BTS Free EMG graphical user interface to verify the consistency of their placement.

Shoulder and elbow kinematics were monitored using an eight-camera optical motion capture system (BTS Smart DX 7000). Eight reflective markers were placed on suitable right and left upper-body landmarks: the processus spinosus of the seventh cervical vertebra, the processus spinosus of the fifth dorsal vertebra, the acromion for the shoulder, the most caudal point on the lateral epicondyle for the elbow, and the most caudal–lateral point on the radial styloid for the wrist.

Protocol

After the electrodes and markers were placed, subjects were asked to perform functional and nonfunctional tasks. These tasks were designed to simulate gestures typical of automotive underbody scenarios (such as cladding, repairing, and bolt tightening) and to represent generic upper-limb movements that may happen in ordinary working conditions (such as reaching for tools or maintaining awkward arm postures for a relatively long time).

Functional Tests

During the functional tests, participants were asked to stand still under a horizontal panel and perform overhead tasks. The panel depicted a cross inside a circle, and its position was adjusted based on the user's height to allow subjects to perform the tasks with the dominant arm elevated (shoulder flexed at ~90° and elbow flexed at ~90°).

Four trials were carried out, in which each subject was asked to retrace the AP part of the cross, the internal medial–lateral (i-ML) part of the cross, the external medial–lateral (e-ML) part of the cross, and the circumference (Figure 3). Each trial consisted of 20 repetitions of the gesture.

Nonfunctional Tests

Nonfunctional tests included three sets of tasks: repetitive reaching movements, static tasks, and quasistatic tasks that are determinants of the complex functional work tasks analyzed.

1) *Repetitive reaching tests*. Each participant was requested to perform reaching movements, starting from a relaxed arm position to a forward-reaching arm position (Figure 3). The arm was considered straight when the shoulder reached 90° in the flexion direction and the elbow was fully extended (0°). A wooden bar was placed vertically in front of the user, with a sign at the height of the user's right acromion. The sign on the bar was used as a target point that participants had to approach more closely each time they repeated the reaching movement. The distance between the vertical bar and the subject was adapted to be equal to the user's arm length. Subjects were asked to perform the task from a sitting position and keep their backs straight. Reaching trials were executed three times: the first with the bar positioned in the external workspace, i.e., 45° medial angle of the arm (external reaching), the second with the bar positioned in front of the right acromion of the user (frontal reaching), and the third with the bar positioned in the internal workspace, i.e., −45° medial angle of the arm (internal reaching). In each condition, subjects were requested to repeat the movements repetitively 12 times at a self-selected pace.
2) *Static test*. Each subject was asked to stand still and keep the right arm in a flexed position (90°), with the elbow fully extended, for 60 s (Figure 3).
3) *Quasistatic test*. Each subject was asked to retrace four arrays of 20 sinewaves on a vertical transparent panel. The panel was vertically regulated to enable alignment between the user's shoulder and the sinusoidal trace. Movements were executed with the arms straight (i.e., shoulder flexed at ~90° and elbow fully extended) and the person standing still (Figure 3). EMG and kinematics data related to the tracking movements of the first and last arrays were recorded, to compare the performance at the beginning and end of the task.

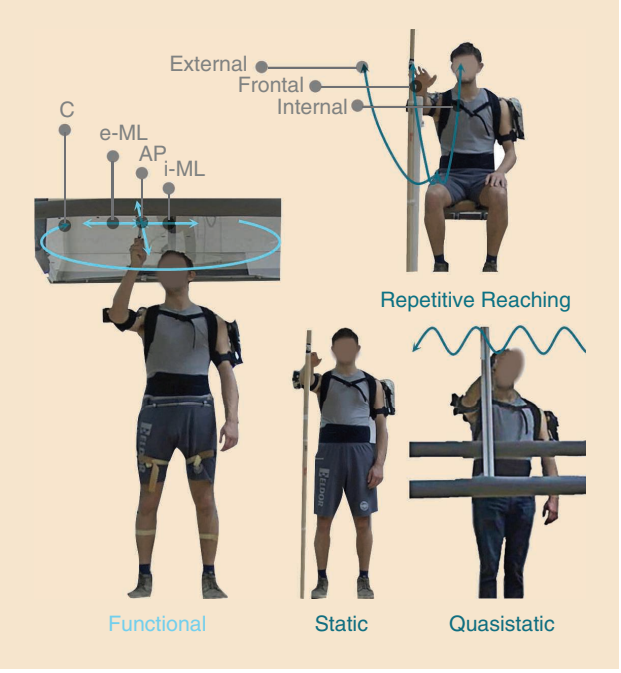

Figure 3. A schematic of the tasks. The image on the left shows functional movements while nonfunctional movements are shown on the right. C: circumference.

Experimental Conditions

Each task was executed under two conditions: without and with the exoskeleton (these conditions are referred in the text as *FREE* and *EXO*, respectively). The order of FREE and EXO conditions was randomized across participants.

Before starting the EXO trials, the level of assistance was selected as the minimum that allowed compensation for about 50% of the estimated gravitational torque of the user's upper-limb [13] (Table 1). The assistive torque is tuned to compensate for about 50% of the estimated gravitational torque weighing on the upper limb (assessed based on weight and height).

Notably, an additional reflective marker was positioned on the proto-MATE back frame in EXO trials. Its purpose was to assess any relative translational movement between the trunk and the frame of the proto-MATE.

Data Analysis

EMG data were sampled at 1,000 Hz. Raw EMG signals were bandpass filtered with a zero-lag, second-order Butterworth filter (frequency range 20–450 Hz) to remove movement artifacts and high-frequency noise. A zero-lag, second-order infinite impulse response notch filter at 50 Hz was applied to

delete the ac interference. Then, EMG signals were rectified, and a zero-lag 100-ms moving average filter was applied to calculate the envelope of the signal (EnEMG).

Kinematics data were sampled at 250 Hz. Raw kinematic data were preprocessed to remove noise and artifacts: a low-pass, zero-lag, fourth-order Butterworth filter was applied, with a cutoff frequency equal to 10 Hz. Missing data in the marker trajectories were estimated using a cubic-spline interpolation method. Joint angles were reconstructed following the method presented in a recent study [14].

Performance Indicators

The average normalized EMG integral, range of movement (ROM), and displacement of the pHMI (pHMId) were extracted from EMG and kinematic signals to quantify the effectiveness of the assistance and evaluate the human–robot kinematic coupling.

Imaging EMG

Four procedures were considered to calculate the imaging EMG (iEMG), according to the different experimental tasks. In functional tasks, the iEMG parameter was calculated in the last set of 12 gestures, manually segmented from the elbow's and shoulder's flexion angle profiles [Figure 4(a)]. In the reaching tasks, kinematics and EMG signals were segmented into cycles (i.e., each cycle was a functional or reaching movement), spanning two consecutive local minima of the shoulder flexion angle [Figure 4(b)].

For each cycle, the time-normalized integral of EnEMG [15] was calculated using

$$\mathrm{iEMG}(i) = \int_0^T \frac{\mathrm{EnEMG}(t)}{T} dt.$$

Moreover, to analyze the effects of the exoskeleton during the assisted phase (i.e., forward arm movement to reach the target) and the unassisted phase (i.e., backward arm movement to return to the relaxed position), the iEMG was calculated separately in both phases. The two parameters are expressed by

$$\mathrm{iEMG}_{\mathrm{Forward}}(i) = \int_0^{T1} \frac{\mathrm{EnEMG}(t)}{T1} dt$$

$$\mathrm{iEMG}_{\mathrm{Backward}}(i) = \int_0^{T2} \frac{\mathrm{EnEMG}(t)}{T2} dt\,,$$

where T1 and T2 are the duration of the forward and backward phases, respectively, of the reaching movement. In static tasks, the iEMG parameter was calculated in the final 50 s of the acquisition [Figure 4(c)]. In quasistatic tasks, the iEMG parameter was calculated in the last set of 15 sinewaves extracted from the shoulder flexion angle profile [Figure 4(d)].

ROM

In all trials, the ROM was calculated as the difference between the maximum and minimum angle values reached during the trial [16].

Table 1. The criteria adopted for the assistive level selection.

	Weight (kg)	Height (m)	Estimated Upper-Limb Weight (kg)	Estimated Gravitational Torque at SJC at 90° (N·m)*	Desired Assistive Torque at 90° (N·m)	Assistive Level (Actual Assistive Torque at 90°, N·m)
Subject 1	97	1.73	4.79	11.56	5.78	Level 4 (5.5 N·m)
Subject 2	82	1.83	4.05	10.07	5.04	Level 3 (4.8 N·m)
Subject 3	70	1.83	3.45	8.65	4.33	Level 2 (3.8 N·m)
Subject 4	70	1.72	3.46	7.04	3.52	Level 1 (3.2 N·m)
Subject 5	75	1.75	3.71	9.49	4.75	Level 3 (4.8 N·m)
Subject 6	59	1.64	2.91	6.15	3.08	Level 1 (3.2 N·m)
Subject 7	88	1.83	4.34	9.83	4.91	Level 3 (4.8 N·m)
Subject 8	57	1.73	2.81	6.37	3.18	Level 1 (3.2 N·m)
Subject 9	71	1.84	3.51	8.46	4.23	Level 2 (3.8 N·m)
Subject 10	62	1.72	3.06	6.46	3.23	Level 1 (3.2 N·m)
Subject 11	58	1.68	2.86	6.48	3.24	Level 1 (3.2 N·m)
Subject 12	84	1.8	4.14	10	5	Level 3 (4.8 N·m)
Subject 13	64	1.62	3.16	7.62	3.81	Level 2 (3.8 N·m)
Subject 14	60	1.78	2.96	6.7	3.35	Level 1 (3.2 N·m)
Subject 15	80	1.84	3.95	8.94	4.47	Level 3 (4.8 N·m)

*The estimated gravitational torque at the shoulder joint center (SJC) at 90° based on [13].

pHMId

In all trials, the pHMId was calculated as the standard deviation of the relative displacement between the marker placed on the exoskeleton and the one placed on the D5 vertebra, following the method described in [16]. This parameter was calculated only during the EXO condition.

Statistical Analysis

Across-subject medians and interquartile ranges of the three performance indicators under the two conditions were calculated and reported for each trial. Statistical analyses were performed using MATLAB software (Math Works Inc.). Pairwise comparisons of the three indicators were performed to assess differences between the FREE and EXO conditions. The Shapiro-Wilk test was used to test the normality of data (α = 0.05). When parameters failed the normality test, the pairwise Wilcoxon signed-rank test ($\alpha = 0.05$) was performed.

Results

Functional Tests

The results of the functional tests are provided in Figure 5. In all tasks (i.e., AP movements, i-ML, e-ML, and circumference), the anterior or medial deltoid, trapezius ascendens, and pectoralis major showed significantly lower activations in the EXO condition compared to the FREE condition (−18 – −42%, $p \leq 0.05$). In addition, in the AP, internal, and e-ML tasks, the shoulder extensor muscles showed significantly lower activations in the EXO condition than in FREE (posterior deltoid −14 to −21%, $p \leq 0.05$; triceps brachii −16 to −20%, $p \leq 0.05$). No significant difference was found in the activation of biceps brachii and latissimus dorsi between the two conditions. No muscles showed higher activations in the EXO condition.

Regarding the kinematics, in AP, i-ML, and e-ML tasks, no significant differences were observed between the EXO and FREE conditions, in all joints. When using the exoskeleton, reduced shoulder abduction–adduction and elbow flexion–ROMs were observed in the circumference task, compared with the FREE condition (−19% and −23%, respectively). The interquartile range of the pHMId resulted in lower than 0.6 mm in all functional trials.

Repetitive Reaching Tests

The results of the nonfunctional reaching tests are reported in Figure 6. In all reaching trials, significant lower activations of the anterior deltoid (−26 – −36%, $p \leq 0.01$) and pectoralis major (−26 – −43%, $p \leq 0.01$) were reported in the EXO condition with respect to the FREE condition. No significant difference was found in the activation of biceps brachii and latissimus dorsi between the two conditions. In addition, lower EMG activity of the trapezius ascendens was reported in the external and internal reaching trials when using the exoskeleton (−18%, $p = 0.011$). In internal reaching trials, the posterior deltoid activation increased in the EXO condition with respect to the FREE condition (+30%, $p \leq 0.05$).

In terms of kinematics, in all reaching tasks, the shoulder flexion–extension (S-FE) ROM was not affected when using the exoskeleton ($p \geq 0.3$). The shoulder abduction–adduction ROM decreased in the EXO condition in the internal reaching trial (−33%, $p = 0.001$), while no significant changes were found in frontal and external reaching tasks. Considering the elbow ROM, significant reductions were found in all tasks (frontal reaching, −35%, $p = 0.0001$; internal reaching, −41%, $p = 0.0001$; and external reaching, −25%, $p = 0.0001$). The interquartile range of the pHMId result was lower than 2 mm.

Static Tasks

Results of static trials are reported in Figure 7. The majority of muscles (anterior deltoid, medial deltoid, trapezius ascendens, triceps brachii, pectoralis major, and latissimus

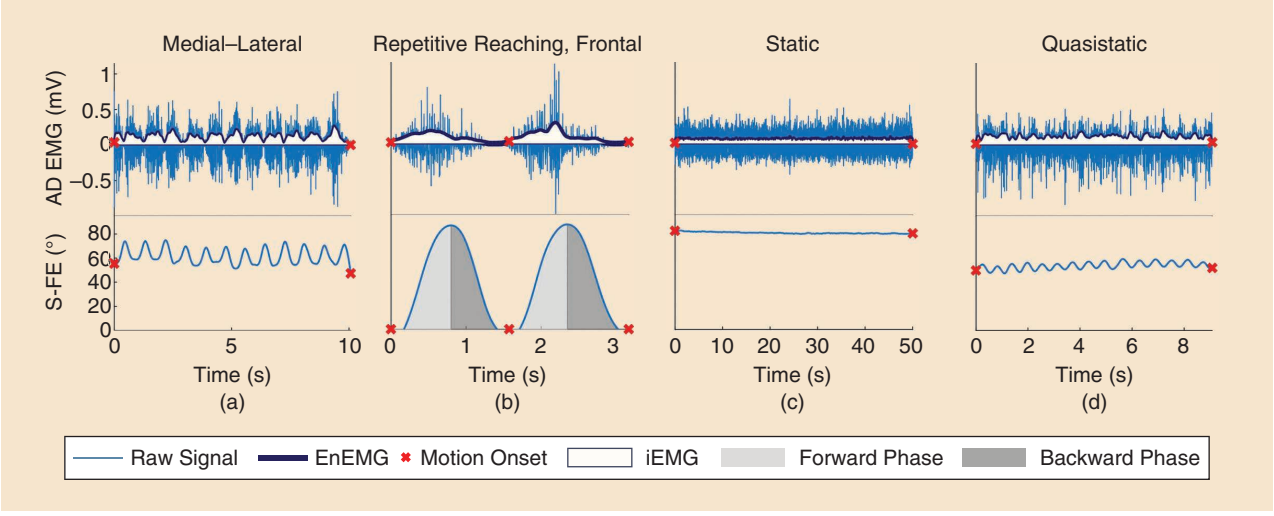

Figure 4. The data analysis and extraction of EMG and ROM parameters. In (a) medial–lateral, (c) static, and (d) quasi-static tasks, the final part of the signals is selected to calculate EMG parameters. (b) The reaching tasks segmentation is based on the shoulder flexion–extension angle (S-FE). EMG parameters are calculated for each cycle. AD: anterior deltoid.

dorsi) significantly reduced their activation level in the EXO condition (observed reductions were in the range of −16 to −35%, $p \leq 0.05$), with the trapezius and pectoralis major showing the highest reductions (−29% and −35%, $p \leq 0.05$ and $p \leq 0.0004$, respectively). The analysis did not reveal any significant differences in the activation of the biceps brachii and posterior deltoid between the FREE and EXO conditions.

In this task, the shoulder and elbow flexion–extension ROMs did not show significant differences between the FREE and EXO conditions, while the shoulder abduction–adduction ROM decreased (−23%, $p = 0.005$).

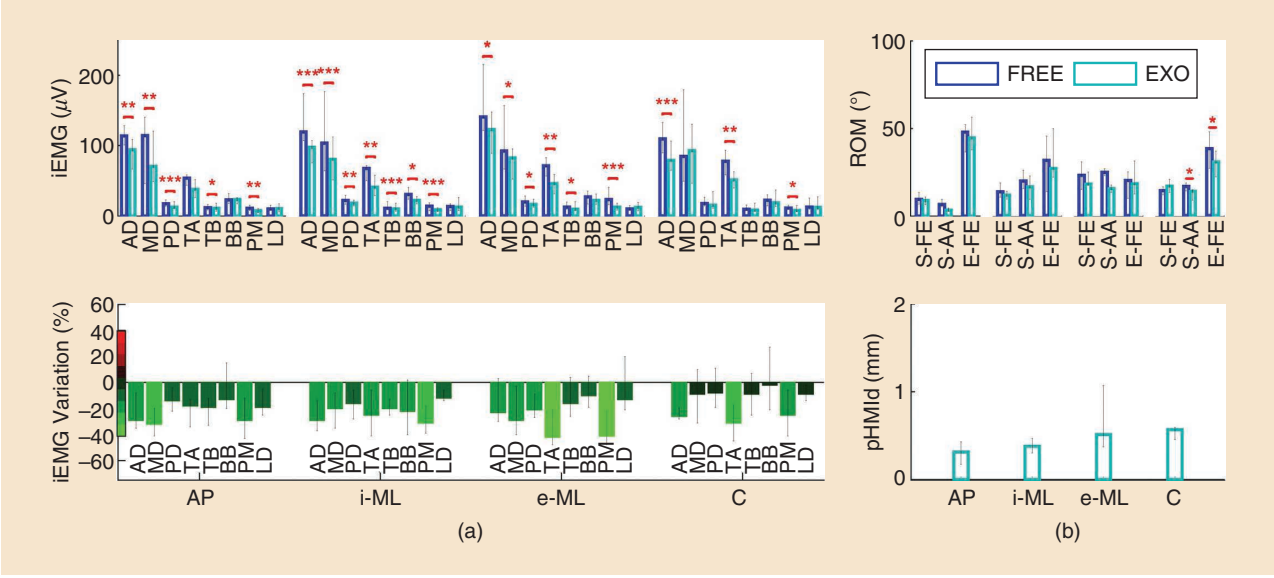

Figure 5. The results for the functional tasks. (a) Muscle activations are reported as iEMG. The average pairwise percentage variations of the iEMG parameter between the FREE (blue) and EXO (light blue) conditions are reported. Red bars indicate increased muscular activity in the EXO with respect to the FREE condition, and green boxes indicate decreased activations. (b) ROMs are reported for S-FE, shoulder abdo-adduction (S-AA), and the elbow flexion extension. The box plots and error bars refer to the intersubject median and interquartile range, respectively. Red asterisks represent statistically significant differences. *: $p \leq 0.05$; **: $p \leq 0.01$; ***: $p \leq 0.001$; AD: anterior deltoid; MD: medial deltoid; PD: posterior deltoid; TA: trapezius ascendens; TB: triceps brachii; BB: biceps brachii; PM: pectoralis major; LD: latissimus dorsi.

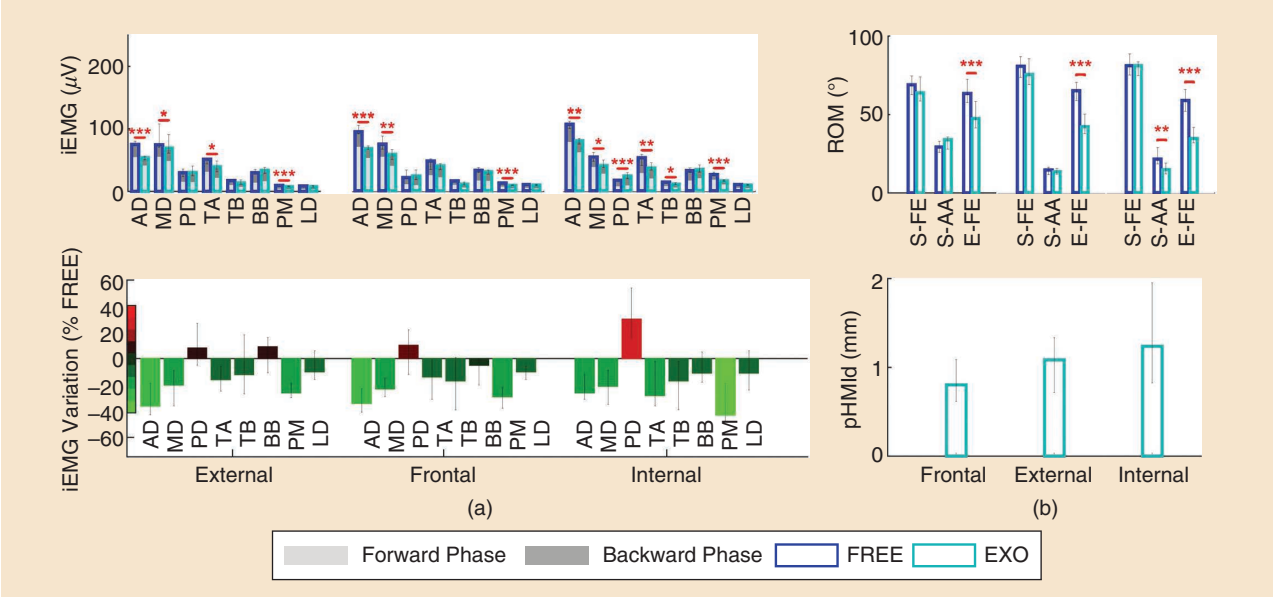

Figure 6. The results for the functional tasks. (a) Muscle activations are reported as iEMG. The average pairwise percentage variations of the iEMG parameter between the FREE (blue) and EXO (light blue) conditions are reported. Red bars indicate increased muscular activity in the EXO with respect to the FREE condition, and green boxes indicate decreased activations. (b) ROMs are reported for S-FE, S-AA, and E-FE. The box plots and error bars refer to the intersubject median and interquartile range, respectively. Red asterisks represent statistically significant differences. *: $p \leq 0.05$; **: $p \leq 0.01$; ***: $p \leq 0.001$.

The interquartile range of the pHMId result was lower than 1 mm.

Quasistatic Tasks

Results of quasistatic trials are reported in Figure 7. Almost all agonist muscles (anterior deltoid, trapezius ascendens, triceps brachii, and pectoralis major) showed a significantly lower activation in the EXO condition compared to the FREE condition (−25%, −29%, −25%, and −40%, respectively; $p \leq 0.05$). No significant difference was found in the activation of the medial deltoid, posterior deltoids, biceps brachii, and latissimus dorsi between the two conditions. The arm kinematics did not show significant alterations due to the use of the exoskeleton, and the interquartile range of the pHMId result was lower than 1 mm.

Discussion

The experimental protocol was designed to investigate the effects of a novel passive, upper-limb exoskeleton on the physical strain of upper-limb muscles and on the human–robot kinematic coupling. Simulated laboratory trials aimed to reproduce overhead underbody assembly tasks (called *functional tasks*) and more generic context-aware reaching movements (here called *nonfunctional tasks*) that may likely occur in assembly lines when workers reach for objects or displace and manipulate tools.

Assessment of the Effects on Muscle Activations

With the objective to provide a comprehensive overview of the effects of the proto-MATE on the glenohumeral and scapular muscles, in this study we investigated eight superficial muscles involved in shoulder girdle movement, including agonist and antagonist groups. The results presented in this study showed that EMG activations of all agonist muscles involved in shoulder flexion, gravity support of the arm, and shoulder stabilization (i.e., the anterior deltoid, medial deltoid, trapezius ascendens, and pectoralis major) had significantly reduced physical strain when using our passive upper-limb exoskeleton.

In all functional trials, we observed remarkable reductions of the anterior deltoid, trapezius ascendens, and pectoralis major activations, ranging between −18% and −42%. Overall, the MATE seemed to unload the physical demand of the main shoulder elevator muscles, in a range that, depending on the trial, varied from −2% to −8% and up to −40%. Such results are in line with other studies, which mostly reported EMG reduced activations of the anterior or medial deltoid and trapezius when performing repetitive overhead tasks with the EksoVest [4] and ShoulderX [6]. In some studies, the resulting variations between EXO and FREE conditions for some muscles were slightly higher than in our assessment; but note that several differences in the experimental protocol (e.g., methods for tuning the assistance, type and duration of the tasks, and loading conditions) can make direct comparison of the variation values complex.

In addition to the positive, expected results on the agonist muscles, we observed significant EMG reductions in the posterior deltoid muscle during functional trials; such unexpected beneficial effects of the device may raise several important considerations regarding the impact long-term use of the device can have. It is well known that the posterior deltoid, together with the rotator cuff muscles, strongly

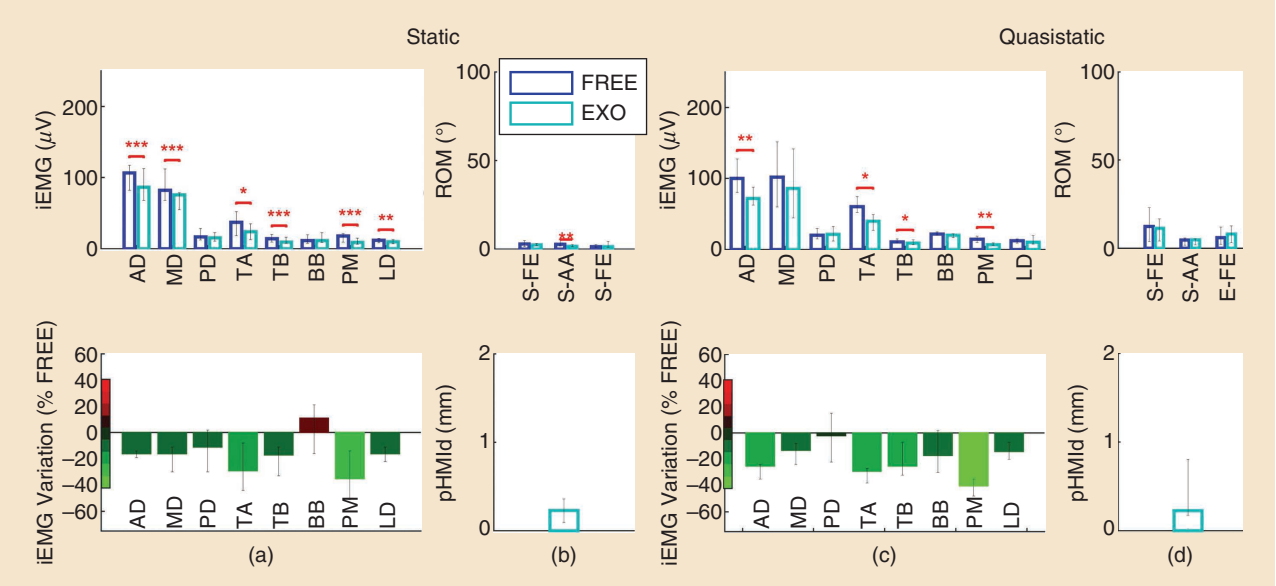

Figure 7. The results in (a) and (b) static and (c) and (d) quasistatic tasks. The muscle activations are reported as iEMG. The average pairwise percentage variations of the iEMG parameter between the FREE (blue) and EXO (light blue) conditions are reported. Red bars indicate increased muscular activity in the EXO with respect to the FREE condition, and green boxes indicate decreased activations. ROMs are reported for S-FE, S-AA, and E-FE. The box plots and error bars refer to the intersubject median and interquartile range, respectively. The red asterisks represent statistically significant differences. *: $p \leq 0.05$; **: $p \leq 0.01$; ***: $p \leq 0.001$.

contributes to providing compressive forces that keep the humeral head centered on the glenoid, particularly stabilizing the humeral head against anterior displacements that occur during static and dynamic arm elevation [17]. The reduced activation of the posterior deltoid in functional tasks may be correlated to a reduced anterior displacement of the humeral head, which likely results from the reduced strain of the flexor and abductor muscle-tendon units. The overall reduced load on the shoulder girdle, i.e., the combined reduced strain of the flexor (anterior deltoid) and extensor (posterior deltoid) muscles when performing overhead tasks, can have long-term effects on the incidence of shoulder tendon disorders.

While functional overhead movements are optimal experimental conditions to verify the beneficial effects of a passive exoskeleton on upper-limb muscles strain, testing the device's effects on context-aware movements was considered crucial to demonstrate the potential beneficial effects in nontask-specific gestures that may be frequently repeated in real working conditions.

In all unfunctional trials, a remarkable and statistically significant decrease of EMG activity was found for several upper-limb muscles that contribute to the elevation of the shoulder. Similar to functional tasks, the most significant reductions were found on the anterior and medial deltoids, pectoralis major, and the trapezius ascendens, with reductions spanning from −16 to −35% in static trials, from −25% to −40% in quasistatic trials, and from −16% to −43% in repetitive reaching tasks. Such significantly reduced EMG activity of most agonist muscles provides evidence of the effectiveness of the device in scenarios where the main working task could be generalized by reaching movement primitives as well (e.g., pick and place tasks, assembly tasks). Compared to functional (overhead) tasks, in most reaching tasks we observed a different behavior of the posterior deltoid muscle, which showed a tendency toward increased activity in EXO compared to the FREE condition (although statistical significance resulted only in the internal reaching task). In these tasks, users were probably actively counteracting the elevation torque provided by the device, exerting an extension force necessary to counteract the inertia-elastic action of the actuation units. The assistance was tuned to compensate for only part of the gravity torque of the arm, with the goal being to reduce such active counteraction behaviors because the residual gravity torque should allow the user to easily move his/her arm back to the resting position without the need to actively work against the assistance. However, it is likely that users were acting eccentrically to decelerate the arm flexion in the forward phase and concentrically accelerate the arm in the backward phase. Clearly, this behavior was evident in highly dynamic trials, for which the forward and backward movements were performed at a quasisteady pace, whereas in less dynamic trials this effect was not reported.

Overall, the latissimus dorsi, which was involved in back extension and lateral flexion as well as in shoulder adduction [18], did not significantly change its electromyographic activity when using the exoskeleton with respect to the normal condition.

In a few cases of external reaching trials, higher (but not significant) activations of the biceps brachii were detected when using the device. This was likely related to the stabilizing action of the muscle on the shoulder and elbow joints, stiffening the elbow against an increased extensor torque, or to an overestimated muscle force exerted to stabilize the shoulder, due to the short adaptation time to the assistance. In fact, the results of this study show the short-term adaptation effects on users who had no prior experience with the tasks being performed or the use of the device. While the results suggest that users were immediately able to modulate their muscle activations to benefit from the assistance, longer training sessions could potentially increase the device's effectiveness.

Unexpected beneficial effects of the device may raise several important considerations regarding the impact long-term use of the device can have.

In addition, in this study we tuned the assistance to a relatively comfortable value (i.e., with the goal to compensate for about 50% of the arm gravity torque) that would allow participants to perform both repetitive and static shoulder flexion movements without being hindered by the exoskeleton. However, finding the optimal task-specific assistive level would likely lead to even better results.

Assessment of the Human–Robot Kinematics Coupling

This study was designed to investigate the human–robot kinematic coupling, by means of two specific metrics: one (the joint ROMs) describing whether wearing the device affects the human joints kinematics and the other (the pHMId) describing the relative movement between the human body and the device, as a global measurement of the good transfer of reaction forces and proper joint alignment [16].

The results showed that the ROMs were not affected by the use of the proto-MATE in functional trials. Particularly, the S-FE results were comparable in the EXO and FREE conditions in all of the functional and nonfunctional trials, providing evidence of the effective human–robot cooperation in the device's main working plane.

In a few static and internal reaching trials, slight changes in the shoulder adduction–abduction ROMs were observed. This could be partly explained by the abducted posture being particularly demanding for shoulder muscles. Participants naturally may have slightly reduced abducted arm postures when working in FREE conditions; conversely, in the EXO condition where a large portion of the arm gravity is

compensated for the system, users may have preferred alternative motor strategies, spontaneously assuming a more abducted position. This could also be a reliable explanation for the reduced elbow ROM reported in all the reaching tasks. Indeed, since the elbow is not assisted by the device, the ROM variation is likely not due to motion constraints induced by the device but rather as a result of alternative movement strategies adopted by the user.

Similar metrics and results were used by S. Kim et al. in [5], who reported no differences in the shoulder flexion angle when wearing the EksoVest and noted slight reductions of the abduction–adduction ROM, likely due to the device encumbrance.

Another relevant issue to consider in properly evaluating the performances of the device is the relative pHMId, which may be representative of possible misalignments between the human and the robot joint axes, potentially inducing joint overload. As expected, in static, quasistatic, and functional tasks, the pHMId results were more stable than in highly dynamic reaching trials. In all trials, the pHMId result was lower than 2 mm. Such a value can be considered acceptable, considering that 11 mm is the maximum relative displacement of a wearable device that will avoid discomfort due to skin irritations or sores [19]. These results are also in line with a similar study from our group based on active pelvis orthosis, which reported maximum pHMId values of 3.2 ± 2.2 mm during walking trials [16].

Limitations of the Study

The results of this study should be interpreted by considering the following three main limitations. First, different from the working population, participants in this study were young and healthy and had no task experience. The findings of this study, while promising, would need to be further proved with actual workers to draw more general conclusions on the device's effectiveness. Even more positive findings could result from experienced workers who are trained to execute the tasks, since their skills should be reflected in the presence of more focused EMG patterns, as outcomes of their trained motor capability. The second limitation is that the trials were carried out in a laboratory setting, where several technical and acceptability issues cannot be considered. Finally, the evaluation metrics were limited to objective measures of muscle activations and human–robot kinematics compatibility; more metrics related to subjective acceptability and usability would give more insights into the device's perceived usefulness. Although very relevant, some studies highlighted that subjective questionnaires submitted to inexperienced young participants may not provide accurate results, so this metric will be considered in future experimentations with workers.

Conclusions

Passive exoskeletons have been introduced into the global market to improve the ergonomic condition of workplaces and promote the well-being of workers exposed to physically demanding tasks. This article investigated the effect of using the proto-MATE on upper-limb muscles and on the human–robot kinematic coupling. Its relevance relies on three main distinctive features. These include the first-time evaluation of the novel exoskeleton proto-MATE, which presents peculiar distinctive characteristics with respect to other unpowered exoskeletons in both structural design and interactions with the user; the comprehensive investigation of the proto-MATE effects on muscles engaged in both shoulder mobility and stabilization; and the inclusion, in the evaluation protocol, of tasks that are representative of the target application (i.e., functional tasks) and antigravitational tasks that generalize nontarget upper-limb movements (nonfunctional tasks).

Overall, results showed that using the proto-MATE can reduce the EMG activations of most upper-limb muscles involved in flexion movements and shoulder stabilization up to 43%. The shoulder abduction–adduction and flexion–extension ROMs were not significantly altered when using the proto-MATE, and the human–robot relative displacement during the tasks was always lower than 2 mm.

These findings indicate that good human–robot kinematic coupling makes the proto-MATE effective for reducing the physical demand of the shoulder girdle by minimizing the transfer of undesired force to the user's musculoskeletal system. Long-term effects of device use on actual workers will be investigated in future works, to study potential implications of a systematic adoption of the MATE on the incidence of WRMDs.

Acknowledgments

Nicola Vitiello and Simona Crea share senior authorship. Matteo Moisé, Luca Morelli, Duane Romo, Giuseppe Colombina, Francesco Giovacchini, Nicola Vitiello, and Simona Crea have interests in the commercial exploitation of the MATE technology. Matteo Moisé, Luca Morelli, Francesco Giovacchini, Nicola Vitiello, and Simona Crea are shareholders of IUVO SRL. Giuseppe Colombina is the chief executive officer of IUVO SRL and an employee of Comau S.p.A. Duane Romo is an employee of Össur. Comau and Össur are shareholders of IUVO.

References

[1] Eurofound, "Sixth European Working Conditions Survey: 2015. Data visualisation," Dublin, UK. [Online]. Available: https://www.eurofound.europa.eu/data/european-working-conditions-survey?locale=EN&dataSource=EWCS2016&media=png&width=740&question=y15_Q88&plot=euBars&countryGroup=linear&subset=agecat_3&subsetValue=All.

[2] E. Iden, "XXI World Congress on Safety and Health at Work 2017—Through the eyes of a delegate," *Occupat. Health South Africa*, vol. 23, no. 6, p. 6, 2017.

[3] J. Grieve and C. R. Dickerson, "Overhead work: Identification of evidence-based exposure guidelines," *Occupat. Ergonom.*, vol. 8, no. 1, pp. 55–66, 2008.

[4] S. Kim, M. A. Nussbaum, M. I. Mokhlespour Esfahani, M. M. Alemi, B. Jia, and E. Rashedi, "Assessing the influence of a passive, upper extremity

exoskeletal vest for tasks requiring arm elevation: Part II—'Unexpected' effects on shoulder motion, balance, and spine loading," *Appl. Ergonom.*, vol. 70, pp. 323–330, July 2018. doi: 10.1016/j.apergo.2018.02.024.
[5] S. Kim, M. A. Nussbaum, M. I. Mokhlespour Esfahani, M. M. Alemi, S. Alabdulkarim, and E. Rashedi, "Assessing the influence of a passive, upper extremity exoskeletal vest for tasks requiring arm elevation: Part I—'Expected' effects on discomfort, shoulder muscle activity, and work task performance," *Appl. Ergonom.*, vol. 70, pp. 315–322, July 2018. doi: 10.1016/j.apergo.2018.02.025.
[6] L. Van Engelhoven, N. Poon, H. Kazerooni, A. Barr, D. Rempel, and C. Harris-Adamson, "Evaluation of an adjustable support shoulder exoskeleton on static and dynamic overhead tasks," in *Proc. Human Factors Ergonom. Soc. Annu. Meeting*, 2018. doi: 10.1177/1541931218621184.
[7] J. Theurel, K. Desbrosses, T. Roux, and A. Savescu, "Physiological consequences of using an upper limb exoskeleton during manual handling tasks," *Appl. Ergonom.*, vol. 67, pp. 211–217, Feb. 2018. doi: 10.1016/j.apergo.2017.10.008.
[8] S. Spada, L. Ghibaudo, S. Gilotta, L. Gastaldi, and M. P. Cavatorta, "Investigation into the applicability of a passive upper-limb exoskeleton in automotive industry," *Procedia Manuf.*, vol. 11, pp. 1255–1262, June 2017. doi: 10.1016/j.promfg.2017.07.252.
[9] G. Colombina, F. Giovacchini, M. Moisè, L. Morelli, and N. Vitiello, "System for assisting an operator in exerting efforts," Korean Patent WO 2019/016629 A1, July 18, 2018.
[10] M. Peat, "Functional anatomy of the shoulder complex," *Phys. Ther*, vol. 66, no. 12, pp. 1855–1865, 1986.
[11] E. Trigili et al., "Design and experimental characterization of a shoulder-elbow exoskeleton with compliant joints for post-stroke rehabilitation," *IEEE/ASME Trans. Mechatronics*, vol. 24, no. 4, pp. 1485–1496, 2019. doi: 10.1109/TMECH.2019.2907465.
[12] H. J. Hermens et al., "SENIAM 8: European recommendations for surface electromyography," Roessingh Research and Development, Enschede, The Netherlands, 2017.
[13] P. de Leva, "Adjustments to Zatsiorsky-Seluyanov's segment inertia parameters," *J. Biomech*, vol. 29, no. 9, pp. 1223–1230, 1996.
[14] E. Pirondini et al., "Evaluation of the effects of the Arm Light Exoskeleton on movement execution and muscle activities: A pilot study on healthy subjects," *J. Neuroeng. Rehab.*, vol. 13, no. 9, 2016. doi: 10.1186/s12984-016-0117-x.
[15] T. Lenzi, S. M. M. De Rossi, N. Vitiello, and M. C. Carrozza, "Intention-based EMG control for powered exoskeletons," *IEEE Trans. Biomed. Eng*, vol. 59, no. 8, pp. 2180–2190, 2012. doi: 10.1109/TBME.2012.2198821.
[16] N. d'Elia et al., "Physical human–robot interaction of an active pelvis orthosis: Toward ergonomic assessment of wearable robots," *J. Neuroeng. Rehabil.*, vol. 14, no. 1, p. 29, 2017.
[17] S. B. Lee and K. N. An, "Dynamic glenohumeral stability provided by three heads of the deltoid muscle," *Clin. Orthop. Relat. Res.*, vol. 400, pp. 40–47, July 2002. doi: 10.1097/00003086-200207000-00006.
[18] N. Bogduk, G. Johnson, and D. Spalding, "The morphology and biomechanics of latissimus dorsi," *Clin. Biomech*, vol. 13, no. 6, pp. 377–385, 1998.
[19] J. Mahmud, C. A. Holt, and S. L. Evans, "An innovative application of a small-scale motion analysis technique to quantify human skin deformation in vivo," *J. Biomech*, vol. 43, no. 5, pp. 1002-1006, 2010.
[20] COMAU. Accessed on: Dec. 14, 2019. [Online]. Available: https://www.comau.com
[21] IUVO. Accessed on: Dec. 14, 2019. [Online]. Available: http://www.iuvo.company
[22] OSSUR. Accessed on: Dec. 14, 2019. [Online]. Available: https://www.ossur.com/corporate/

Ilaria Pacifico, The BioRobotics Institute, Scuola Superiore Sant'Anna, Pisa, Italy. Email: ilaria.pacifico@santannapisa.it.

Alessandro Scano, Institute of Intelligent Industrial Systems and Technologies for Advanced Manufacturing, Milan, Italy. Email: alessandro.scano@stiima.cnr.it.

Eleonora Guanziroli, Villa Beretta Rehabilitation Center, Valduce Hospital, Lecco, Italy. Email: eleonora.guanziroli@gmail.com.

Matteo Moisé, IUVO SRL, Pisa, Italy. Email: matteo.moise@iuvo.company.

Luca Morelli, IUVO SRL, Pisa, Italy. Email: luca.morelli@iuvo.company.

Andrea Chiavenna, Villa Beretta Rehabilitation Center, Valduce Hospital, Lecco, Italy. Email: chiavenna.andrea@gmail.com.

Duane Romo, New Technology Orthopedics Research and Development, Össur Americas, Foothill Ranch, California. Email: dromo@ossur.com.

Stefania Spada, Fiat Chrysler Automobiles, Turin, Italy. Email: stefania.spada@fcagroup.com.

Giuseppe Colombina, IUVO SRL, Pisa, Italy, and Comau S.p.A., Turin, Italy. Email: giuseppe.colombina@comau.com.

Franco Molteni, Villa Beretta Rehabilitation Center, Valduce Hospital, Lecco, Italy. Email: fmolteni@valduce.it.

Francesco Giovacchini, IUVO SRL, Pisa, Italy. Email: francesco.giovacchini@iuvo.company.

Nicola Vitiello, The BioRobotics Institute, Scuola Superiore Sant'Anna, Pisa, Italy; IRCCS Fondazione Don Gnocchi, Milan, Italy; and Department of Excellence in Robotics & AI, Scuola Superiore Sant'Anna. Email: nicola.vitiello@santannapisa.it.

Simona Crea, The BioRobotics Institute, Scuola Superiore Sant'Anna, Pisa, Italy; IRCCS Fondazione Don Gnocchi, Milan, Italy; and Department of Excellence in Robotics & AI, Scuola Superiore Sant'Anna. Email: simona.crea@santannapisa.it.